

Title	Large-scale spatiotemporal modeling of travel behavior, electric vehicle charging demand, and flexibility based on human mobility big data	
Author(s)	Yamaguchi, Yohei; Ochi, Yudai; Ohara, Ryotaro et al.	
Citation	Energy. 2025, 335, p. 137804	
Version Type	VoR	
URL	https://hdl.handle.net/11094/102784	
rights	This article is licensed under a Creative Commons Attribution-NonCommercial 4.0 International License.	
Note		

The University of Osaka Institutional Knowledge Archive : OUKA

https://ir.library.osaka-u.ac.jp/

The University of Osaka



Contents lists available at ScienceDirect

Energy

journal homepage: www.elsevier.com/locate/energy



Large-scale spatiotemporal modeling of travel behavior, electric vehicle charging demand, and flexibility based on human mobility big data

Yohei Yamaguchi * ©, Yudai Ochi, Ryotaro Ohara, Hideaki Uchida ©, Shinya Yoshizawa, Katsuya Sakai ©, Yutaka Ota, Yoshiyuki Shimoda ©

Graduate School of Engineering, The University of Osaka, M3 Building, 2-1 Yamadaoka, Suita, Japan

ARTICLE INFO

Handling Editor: X Ou

Keywords:
Electric vehicle
Usage modeling
Demand flexibility
Location log
Human mobility analysis
Power system planning

ABSTRACT

The rapid growth of electric vehicles (EVs) and renewable energy has increased the importance of detailed power system planning at multiple scales ranging from local distribution networks to macro-level generation capacity and operations. To maximize the contribution of EVs to decarbonization and system transitions, high spatio-temporal data on EV charging demand and flexibility applicable at multiple scales would be effective. Previous research has established useful modeling approaches. However, limitations to expressing macro and local characteristics simultaneously remain. To address this deficiency, this study developed a data-driven workflow to extract vehicle usage profiles from human mobility big data collected from mobile devices to quantify vehicle usage, EV charging demand, and flexibility on a large scale at a high spatiotemporal resolution. The application to entire Japan showed that if all the private vehicles are electric, uncontrolled home charging would reach a maximum of 25 GW. EVs have significant flexibility potential through smart charging and vehicle-to-grid operations. The 1 km-mesh-resolution data showed that activity patterns, demand, and flexibility vary considerably depending on the accessibility to public transportation. The established method can provide high spatiotemporal resolution EV data for various purposes and also allows for iterative studies that integrate local and macro-level power systems.

1. Introduction

Electrifying vehicles is essential to reducing carbon dioxide emissions. The expansion of electric vehicles (EVs) use may pose challenges for the capacity management and operation of power generation and distribution systems [1–3]. Moreover, smart charging and vehicle-to-grid (V2G) operations provide solutions to these problems and contribute to mitigating the impacts of a large-scale deployment of renewable energy sources such as solar photovoltaic and wind power generation through demand response and virtual power plants [4–6]. To address these challenges, models are required that can estimate the EV charging demand and its flexibility under EV ownership and charging option scenarios [7–9]. Such models are particularly effective when the EV penetration is low and real-world data are insufficient.

However, conventional spatiotemporal approaches for modeling EV usage patterns have limitations on simultaneously representing aggregated features of the demand and flexibility for electricity generation systems on a large scale and local features for power distribution systems

at a high spatiotemporal resolution. Models with such capability may help smooth power system transitions by enabling the testing of strategies for various purposes and conducting iterative studies that integrate local and macro-level power systems. To fill the gap, this study develops a data-driven EV usage model based on location log big data collected from mobile devices.

1.1. Related works

Diana et al. [7] classified EV usage modeling approaches into three categories in a systematic review: 1) summary travel statistics models (STSMs) that develop summary statistics or empirical distributions to generate deterministic or stochastic vehicle use patterns, 2) models based on entire activity travel schedules (direct use of observed activity travel schedules (DUOATS) and proper activity based models (ABMs)), and 3) Markov chain models (MCMs) that represent the stochastic characteristic of vehicle state transition when driving or parked at home or other places. STSM has limitations in terms of expressing spatial and

^{*} Corresponding author. Graduate School of Engineering, The University of Osaka; Room 320, M3 Building, 2-1 Yamada-oka, Suita, Osaka, 565-0871, Japan. E-mail address: yohei@see.eng.osaka-u.ac.jp (Y. Yamaguchi).

temporal details. MCM is developed based on observed EV usage data. The review by Yaghoubi et al. [57] highlighted the development of data-driven machine learning, deep learning, and ensemble methods using observed data in recent years. MCM and these data-driven methods are ineffective where EV penetration is low as these have been developed in data-rich environments. DOUATS and ABM are generally developed based on travel diaries collected from travel surveys, or using location log data. DOUATS uses fixed travel schedules from observations and is less flexible than an ABM that defines agents performing travel activities stochastically considering features characterized by input data.

Considering heterogeneous spatiotemporal characteristics helps represent realistic EV usage patterns [8]. ABM has progressed significantly in this regard. Mu et al. [10] developed an ABM with a high spatiotemporal resolution by considering a detailed origine-destination (OD) matrix. Mangipinto et al. [11] modeled the EV charging demand of 28 European countries and showed that the hourly patterns vary significantly by country owing to the weather and user behavior. Lin et al. [12] developed an ABM that explicitly considers trip chains, which distinguish between travel purposes and the types of places visited. Jahangir et al. [13] proposed a neural network model of the travel distance based on the relationship with the departure and arrival times. Zhang et al. [14] considered the variation in activity with individuals' demographics and location types. Pareschi et al. [15] showed that travel survey data effectively represent the mobility behavior of EVs. Liu et al. [16] developed a model representing the population of the Atlanta metropolitan area and quantified the spatiotemporal distribution of the charging demand. Gschwendtner et al. [17] applied a high spatiotemporal resolution ABM (the Multi-Agent Transportation Simulation (MATSim)) to three Swiss cities representing urban, suburban, and rural areas. They showed that the charging demand and flexibility vary significantly depending on the region and type of location. Szinai et al. [18] and Wu et al. [19] applied MATSim to California, USA, and conducted an integrated analysis of the power system and charging station planning. Vollmuth et al. [5] applied this model to show that significant cost advantages could be achieved. POLARIS is acknowledged as a highly advanced ABM transportation simulation with high temporal resolution and fidelity in behavioral representation compared with MATSim. This enables detailed representation of user behavior in various contexts [23,24]. Integrated analyses with residential buildings have been also performed by combining models of in-home activity and the resultant household energy demand [20-22].

Notwithstanding the important knowledge gained by ABMs, several shortcomings in representing the spatiotemporal characteristics of EV usage have been identified [25]. Furthermore, owing to the complexity of model development, the spatial scale of model application is usually limited to cities or metropolitan areas. In addition, the highest level of spatial resolution is limited to cities or marginally smaller areas. These are insufficient for power system planning at multiple scales.

With the current spread of smartphones, an alternative approach using human mobility big data that utilizes smartphone location logs has been proposed. Liu and Dong [26] established a method for extracting human mobility patterns while identifying the homes, workplaces, and other locations of mobile phone users using a density-based spatial clustering algorithm. Martin et al. [27] proposed a standardized data processing pipeline for location log data. Several studies related to EVs have been conducted. Xu et al. [28] developed an ABM using call detail records collected from 1.39 million mobile phone users in the San Francisco Bay Area. Zhang et al. [29] analyzed location data collected from 1.6 million mobile phone users to assess the potential for widespread EV adoption. Zhang et al. [30] used the same data to analyze the variations in EV charging and residential electricity demand profiles owing to population aging.

1.2. Research gap and contribution

Research using location log big data shows considerable potential for application to more comprehensive and detailed EV charging and flexibility analysis. Because the trajectories of individual users are available, it is feasible to consider the spatiotemporal characteristics of EV usage, charging demand, and local constraints on flexibility application. Furthermore, the aggregated demand can be expressed as the sum of individual demands. This can potentially be applied for an integrated analysis at multiple scales. However, research has not been conducted using location log big data for analyzing EV usage, charging demand, and flexibility on a large scale with a high spatiotemporal resolution. A reason for this is that commercially available large-scale location log data is collected using simple location information receivers installed in mobile devices. The data contains a large margin of error, and the frequency of data acquisition varies. These conditions hinder the accurate extraction of vehicle usage. Thus, a workflow addressing these issues should be established.

This study aims to establish a workflow to extract vehicle usage from location log big data and model EV usage, charging demand, and flexibility that can be obtained by smart charging and V2G operation on a large scale at a high spatiotemporal resolution. This research makes two contributions. First, it establishes a workflow to apply low-quality location log data to EV usage modeling. Second, it presents a data-driven DOUATS approach that can provide EV usage data effective for both macro- and local-levels simultaneously under certain EV ownership and charging option scenarios.

1.3. Structure of the paper

Section 2 describes the proposed framework and data used in this study. Section 3 presents the results. This is followed by a discussion in Section 4 and the conclusions in Section 5.

2. Method

In this study, we applied location log data collected from mobile devices in Japan using location-based services provided by the company Agoop. The data was collected from 1.48 million devices, approximately 0.1 % of Japan's total population. Each device has a unique ID that can be used to monitor its trajectory.

Fig. 1 shows the process of estimating the EV usage, charging demand, and flexibility. After pre-processing, the location logs are classified into two types: stay logs recorded while staying at a random location, and movement logs obtained while moving by means of transportation. The travel modes in movement logs are then identified as car, train, walking, and others. Using stay logs, the areas where the user stayed are identified and called spots. A spot is selected for each users' living and working areas using a 1 km mesh. These classification processes are implemented using machine learning techniques. Continuous movement logs between spots are called trips. For user trips by car, the demand for EV charging and the flexibility that can be provided by smart charging and V2G are quantified based on scenarios. In this study, we considered only EV charging and V2G operation while users were staying in their living area.

2.1. Location log data

2.1.1. Data

The data contained in the location logs from Agoop [31] are shown in Table 1. The location coordinates specified by the latitude and longitude of the device are provided with a timestamp. The logs include the accuracy, which indicates the scale of potential errors. The 100-m mesh code of the device's location is also provided. The device is identified by a unique ID, and the trajectory of the device's location can be monitored. This study used data collected from 1.48 million devices over a 12-day

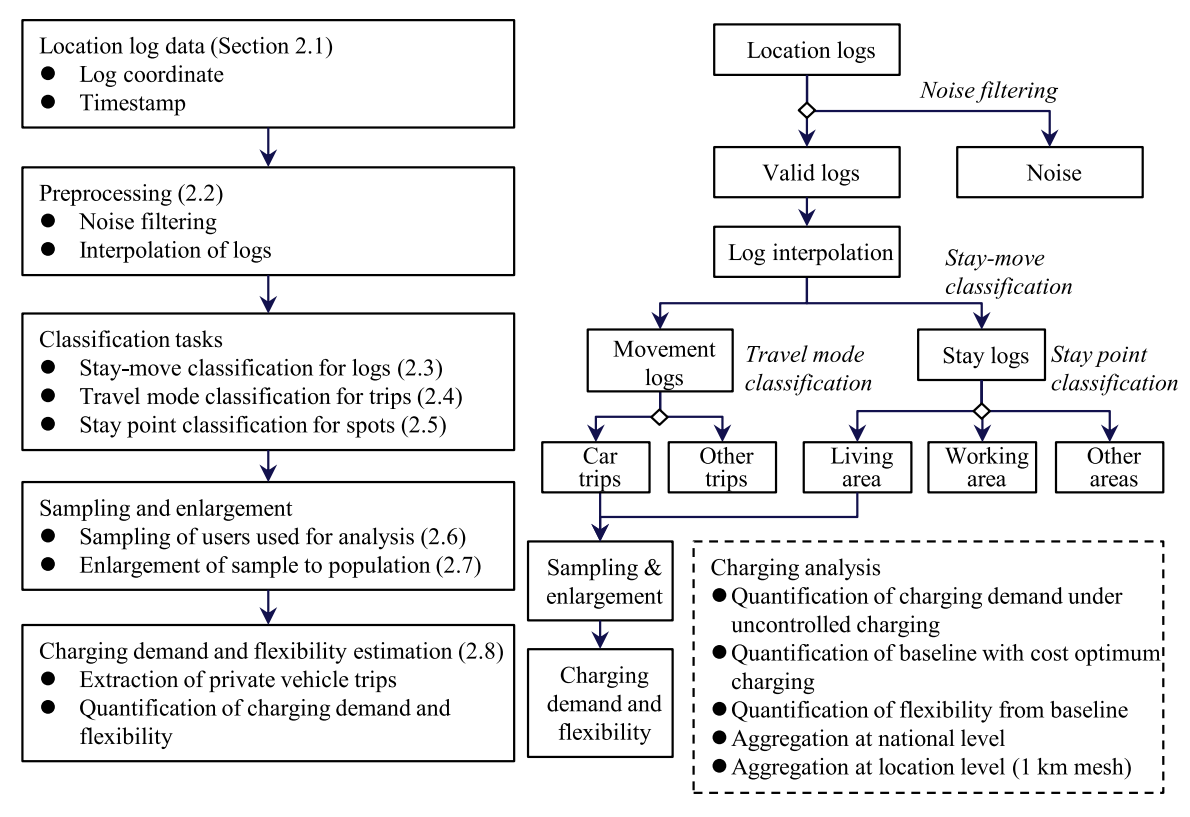


Fig. 1. Developed workflow.

Table 1 Attributes of the location logs.

Attributes	Description
Location coordinate	The latitude and longitude in the World Geodetic System (WGS84) with six decimal places of precision.
Timestamp	The date and time when the log was obtained. The timestamp is
Accuracy	recorded with a minimum resolution of minutes. Horizontal accuracy of the log. In the case of data collected from
	Android devices, this is the radius of the circle that has a 68 % probability of containing the point indicated by the acquired log.
	The definition of horizontal accuracy for iOS data is not
	disclosed.
100 m mesh code	A 100 m mesh that includes the location indicated in the log. The
	mesh is based on the 1/10 subdivision of the third mesh defined
	by the Ministry of Land, Infrastructure, Transport and Tourism.
OS	The operating system of the device owned by the user.

period from October 24 to November 4, 2019. No user demographic information is available. Owing to privacy concerns, the logs near home and workplace are not available.

The location logs were collected from Android and iOS devices that record at different frequencies. Android devices typically collect location logs at fixed time intervals. Meanwhile, iOS devices collect logs more frequently when the user is moving and less frequently otherwise. Furthermore, logs collected from iOS devices generally have a time lag when reading the location signal at the start of movement. The recording frequency is also affected by the device's app settings.

Fig. 2 shows (a) the cumulative frequency distributions of intervals between consecutive logs for all location logs, and (b) those of average log intervals for each user. Fig. 2(a) indicates that most of the logs collected from the iOS and Android devices were recorded within 15 min of the previous log. In Fig. 2(b), approximately 30 % of users have an average of 60 min or more, i.e., one log per hour on average, indicating that there are many users whose logs were recorded infrequently.

2.1.2. Annotation

Annotated data were prepared to train and evaluate the machine learning models developed in the classification processes. 1,500 Android users and 1,500 iOS users were selected randomly. In the manual annotation process, the logs contained in the user's movement trajectory were plotted on map tiles and satellite photograph tiles in conjunction with a timeline. Furthermore, the state of stay/movement or the selected travel mode was determined for each log. First, if logs were recorded continuously in the same location, the user was determined as staying there. Any other behavior was determined as movement. For the stay logs, we considered the frequency of visits, arrival and departure times, length of stay, and characteristics of the area (such as residential area, office district, and factory zone) to label the type of place where the user was staying (living area, working area, and others). For the logs labeled as movement, we rationally determined the travel mode (car, walking, train, and others) by considering the speed of movement and the relationship with the road network and railway lines.

2.2. Preprocessing

2.2.1. Noise filtering

The location log contains errors caused by various factors such as signal reflection and the absence of nearby base stations. If the error is large, the distance between consecutive logs becomes unnaturally large (in the scale of tens of kilometers). To remove erroneous logs, we applied anomaly detection based on heuristics [32]. In this method, logs that start from a certain log, leave the vicinity of that log, and then return within a short time are considered as noise and are removed.

2.2.2. Interpolation

Because the interval between logs in the location log data is not constant, we linearly interpolated consecutive logs to convert these into 1 min intervals.

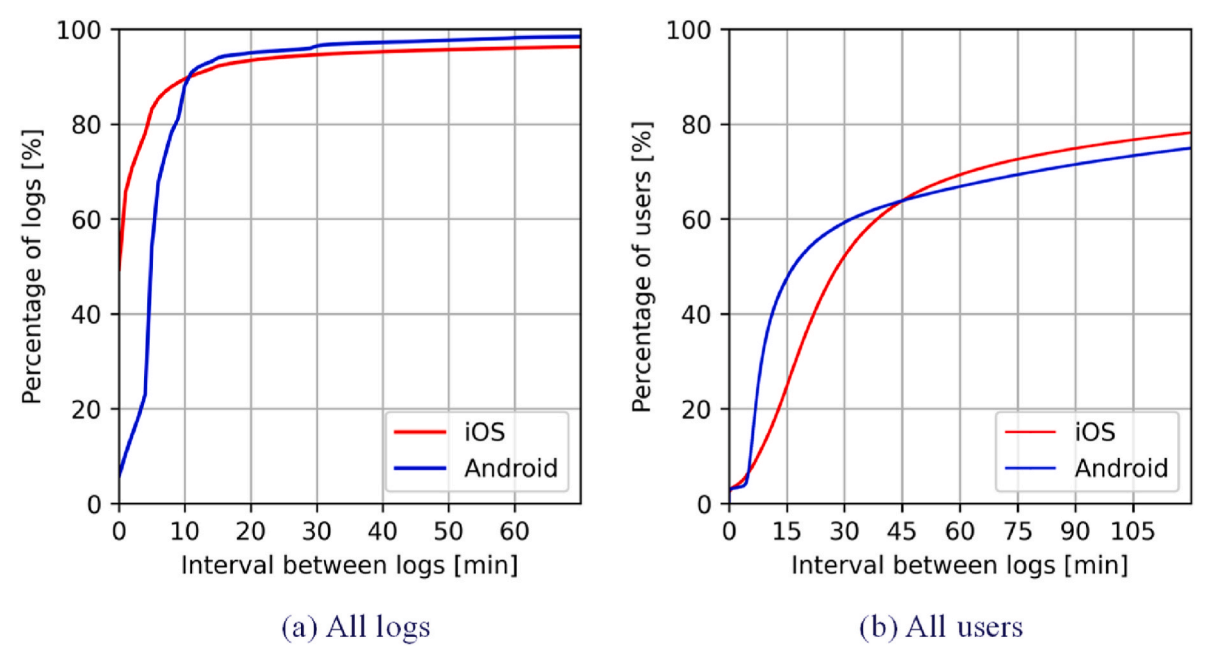


Fig. 2. Distribution of recorded intervals. (a) shows those of all logs, and (b) shows those of the average interval between logs for each user.

2.3. Stay-move classification

To classify the stay logs and movement logs, a density-based spatial clustering algorithm, DBSCAN-TE [33], was applied to the interpolated trajectory data. When an individual is staying at a location, multiple consecutive logs are detected as being located nearby. A group of consecutive logs is identified as a cluster and classified as stay logs. When an individual is moving, the distance between logs is identified. We added to the two processes explained in Supplementary Material A for adapting the characteristics of the low-quality location log data.

2.4. Travel mode classification

For the movement log, XGBoost identified the travel mode by considering whether the user traveled by car, on foot, by train, or by other means (e.g., boat or plane). Bicycles were included in the walking category. For developing the classification models for iOS and Android, 80 % of the annotated data was used to train the classification models. The remaining 20 % was used for validation. Appendix A.1 describes the considered features.

As a preliminary process, trips consisting of at least three logs were labeled as high-quality trips, and the remaining were labeled as low-quality trips. We classified the travel modes for high-quality trips before classifying those for low-quality trips. When classifying the travel modes of low-quality trips, we used the estimated travel modes of the high-quality trips before and after these as features.

In addition, we distinguished bus trips from other vehicle trips. We considered the first and final movements between leaving from and returning to the living area by car to be non-bus travel. This is because we assumed that logs of walking from the living area to the bus stop and vice versa were recorded.

2.5. Stay point classification

After classifying the movement logs and stay logs, spots (where the user stayed) were identified by applying DBSCAN. Then, the living and working areas were selected. Although the locations of homes and workplaces have been deleted from the log data (see Section 2.1.1), it is reasonable that many interpolation logs are within the vicinity where individuals spend a considerable amount of time. A 1 km mesh was

selected with the highest probability for living, whereas working area was selected for each individual if the probability was higher than 50 %. The probability was estimated by XGBoost for each mesh of identified spots. Appendix A.2 explains the classification in detail.

2.6. Sampling

This process excludes users who may introduce errors in the estimation of vehicle energy consumption, based on the upper and lower limits of the parameters listed in Table 2. For various reasons, the actual movement and the trajectory do not match in certain cases. For example, the following would involve underestimation of the distance traveled: users who have not turned on the location information function on their smartphone and therefore do not have sufficient location information, and users who have left their smartphone at home and gone out. These users showed high average values at the log recording intervals shown in Fig. 2(b). Meanwhile, users who have a high frequency of logs with large location measurement errors over a short period of time would have their distance traveled overestimated because the noise cannot be identified in the noise removal process. A similar phenomenon can also be observed for users using an application to conceal their location information. Supplementary Material D shows the distributions of the selected parameters to justify their selection.

Table 2 Parameters used to remove outlier users.

Definition		Limit	Unit	Value
Location	The difference between the recorded position and estimated position	Upper	% ^b	30
uncertainty ^a		Lower	% ^b	26
Proportion of	Proportion of movement logs in	Upper	% ^b	0.01
movement logs	trajectory data	Lower	% ^b	16.0
Number of logs	Number of logs per user	Lower	% ^b	47
Logged days	Number of days in which logs were recorded	Lower	Days	10

^a The location uncertainty represents the average distance between the observed latitude or longitude and the latitude or longitude estimated from the previous and following logs for all the logs in the trajectory data (see Supplementary Material C).

^b The "%" mark indicates the percentage of users excluded when using the highest value as the upper limit and the lowest value as the lower limit.

The upper and lower limits of the parameters were adjusted using Bayesian optimization so that the distance traveled per individual per day in each prefecture could be compared with the National Road and Street Traffic Conditions Survey [34]. The values that minimized the root mean square error (RMSE) for each parameter were selected. As a result of selecting users by these parameters, the number of individuals targeted for estimation was 212,990. The RMSE was 3.51 km/day/vehicle.

2.7. Enlargement to the population

The estimated charging demand of users was multiplied by the expansion rate and expanded to the total population. Fig. 3 shows the distribution of the expansion rate of municipalities. The rate was calculated by dividing the number of private vehicles owned in each municipality [35,36] by the number of private passenger car users. Municipalities with fewer than five users were combined with neighboring areas based on the prefectural assembly election districts.

2.8. Operation of battery

In this study, we analyzed the temporal and spatial distribution of the charging demand. The assumption was that all the private vehicles in Japan would be replaced with EVs. In this estimation, we assumed that the vehicle power efficiency was 7 km/kWh and that the charging power was 6 kW. We also assumed that charging was not controlled and that all the vehicles would be charged immediately after the users return to their living area. For simplicity, we assumed that the battery capacity is equal to the maximum cumulative power use with uncontrolled charging during the period.

We also calculated the flexibility of charging and discharging. First, we determined the baseline charging schedule that minimizes the charging costs by mixed integer linear programming [37,38] considering the wholesale electricity price for that period of the Japan Electric Power Exchange [39]. Then, we calculated the number of EVs that can be charged or discharged continuously over a certain period of time. We multiplied the number of EVs that can be charged or discharged by the rated power of the charger to obtain the potential flexibility of electricity. In this study, we assumed that the time for continuous charging and discharging would be 1 h, 2 h, 3 h, or 6 h. EVs providing flexibility were defined as those staying in living areas with all travel demands satisfied and a state of charge (SOC) between 20 % and 100 % after charging and discharging.

This study only considered private vehicles and home charging. We considered vehicle trips that do not return to the user's living area and rather depart from and return to the user's working area to be commercial vehicle trips.

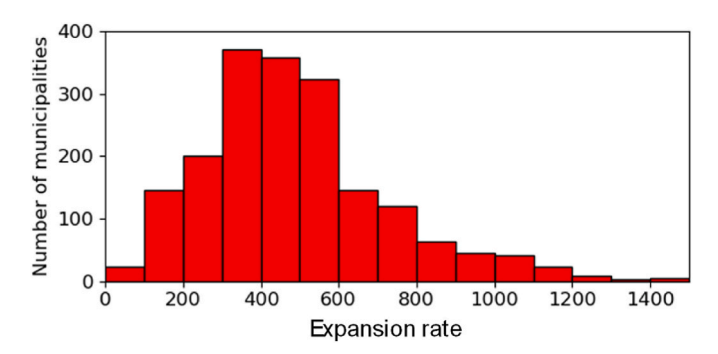


Fig. 3. Distribution of expansion rate. The vertical axis shows the number of 1 km mesh squares with the expansion rate shown on the horizontal axis (intervals of 100).

3. Result

3.1. Log classifications

Fig. 4 shows the distribution of stay logs, divided into living area, working area, and other spots. Fig. 5 shows the results of classifying movement logs by mode of transportation, divided into car, walking, train, and others. As shown in the figures, the stay logs cover entire Japan. However, there are fewer logs in areas with low population density. Supplementary Material E presents an example of the classification results for a user to demonstrate the classification processes.

3.2. Validation

3.2.1. Classification tasks

We evaluated the classification tasks using annotated test data. Table 3 lists the accuracies and F-1 scores of the classification processes. The lowest F-1 score of 0.76 was detected in iOS for the classification of living areas. In general, for GPS trajectory classification tasks, accuracies or F-1 scores exceeding 80 % are commonly considered as being indicative of high performance, and scores above 90 % are evaluated as representing significantly high classification accuracy [40]. Therefore, our results indicated high model performance. As mentioned earlier, iOS devices record logs when the user is staying at a location. Therefore, when iOS users start moving, certain misclassifications are observed owing to insufficient logs. Consequently, the length of stay could not be calculated accurately for certain places. By the same criteria, the scores are sufficiently reasonable.

3.2.2. Average distance traveled by car and energy consumption

To verify the travel distance obtained from trajectory data, we used data from the National Road and Street Traffic Conditions Survey [34]. These data include the average distance traveled by private vehicles in a day. The aggregated values are available for only 10 regions in Japan, which are made up of multiple prefectures. Fig. 6(a) shows the estimated result fitted well.

To verify the estimated energy consumption, we used data of the household consumption of gasoline for private passenger cars in the transportation sector described in the general national energy statistics [41]. To estimate the amount of gasoline consumed from location logs, we divided the distance traveled by the average JC08 mode fuel efficiency in 2019 (22.6 km/L) and multiplied it by the calorific value of gasoline (33.36 MJ/L) [42]. Fig. 6(b) shows the result. The model estimation agreed well (RMSE = 12 PJ/year).

3.3. Estimation of charging demand with uncontrolled charging

Fig. 7 shows the cumulative distribution of battery capacity required for uncontrolled charging during the twelve days. As shown in the figure, most of the distances traveled by users were less than 350 km (equivalent to 50 kWh of battery capacity) and can be supported by major EVs sold worldwide.

Fig. 8 shows the average daily charging demand per household in the 1 km mesh across Japan. The gray areas indicate locations where sufficient data is not available. The charging demand per household is the lowest in the central parts of the Tokyo, Nagoya, and Osaka metropolitan areas, and higher in the suburbs. The demand is low in the central parts owing to convenient access to public transportation. In suburban and rural areas, individuals drive more frequently and travel longer distances. Therefore, the demand tends to increase in a concentric pattern around these areas.

Fig. 9 shows the spatial and temporal distribution of charging demand per household in each 1 km mesh in central Japan's major metropolitan areas (Tokyo, Nagoya, and Osaka) at 0:00, 6:00, 12:00 and 18:00 on Saturday, November 2. Due to uncontrolled charging, the demand for charging at 6:00 is very low. Peak demand occurs at 18:00

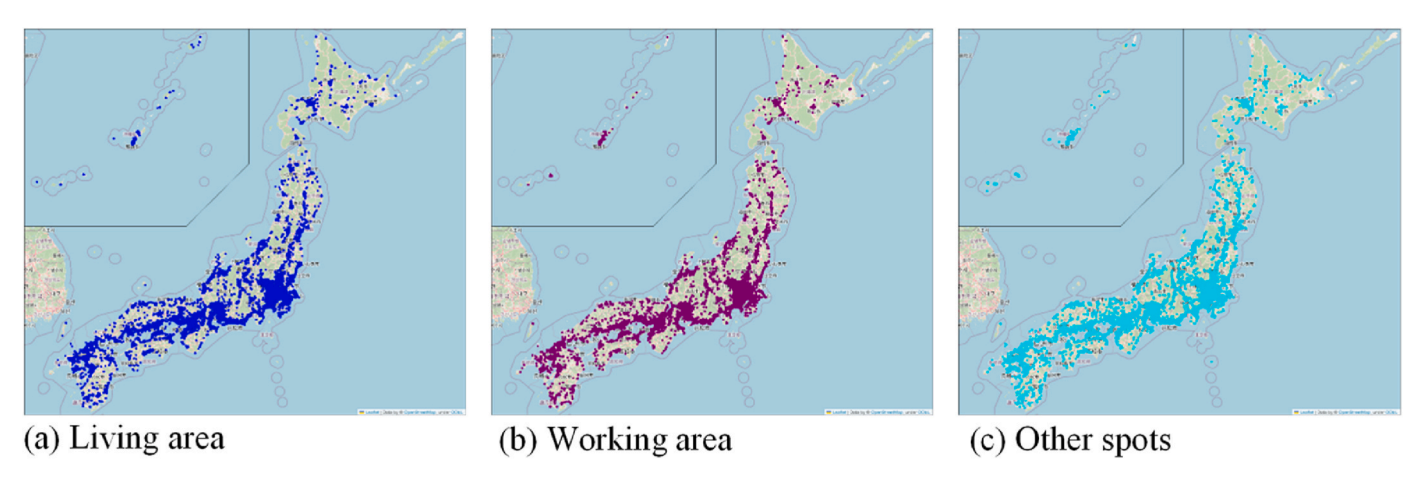


Fig. 4. Locations of stay logs observed in (a) living area, (b) working area, and (c) other spots.

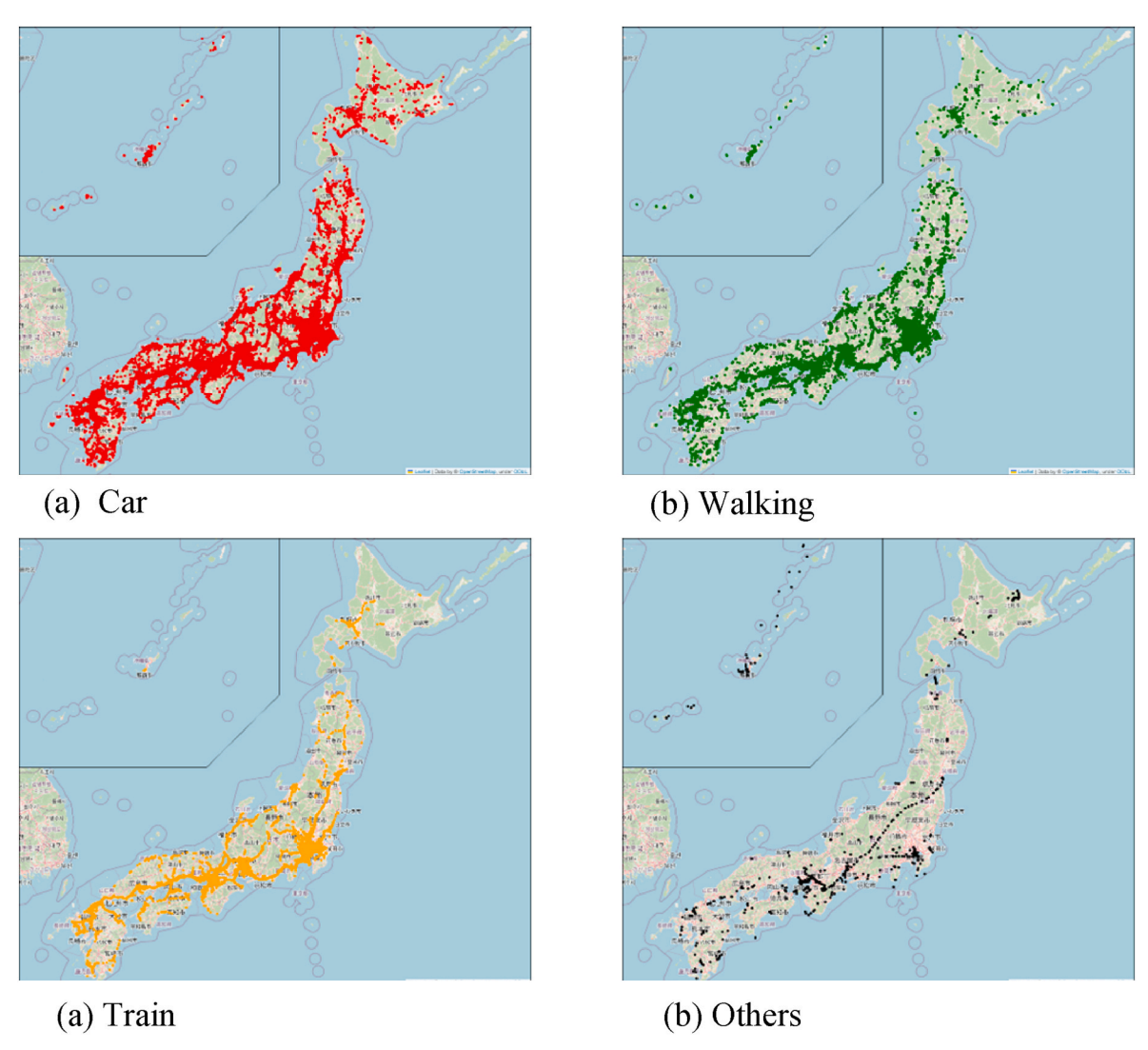


Fig. 5. Travel mode classification result: (a) car, (b) walking, (c) rail/train, and (d) other modes.

relative to the other time periods.

Fig. 10 shows the time series patterns of the total charging demand in Japan and the charging demand per household over time. The peak demand is observed around 19:00, with a total of approximately 26 GW and a per household value of 0.5 kW. This implies that approximately

1/12 of all EVs are being charged during peak time. The peak hours are shorter on weekdays than on holidays. However, the peak demand is approximately equal on all days.

The evening peak coincides with the timing of peak residential electricity demand. Thus, it could have an adverse impact on power

Table 3 Accuracies and F-1 scores of the classification models.

Classification process	os	Accuracy	F-1 score
Stay-move classification	Android	0.96	0.87
	iOS	0.87	0.90
Travel mode	Android	0.88	0.91
classification	iOS	0.91	0.94
Living area estimation	Android	0.99	0.97
	iOS	0.90	0.76
Working area estimation	Android	0.99	0.96
_	iOS	0.99	0.92

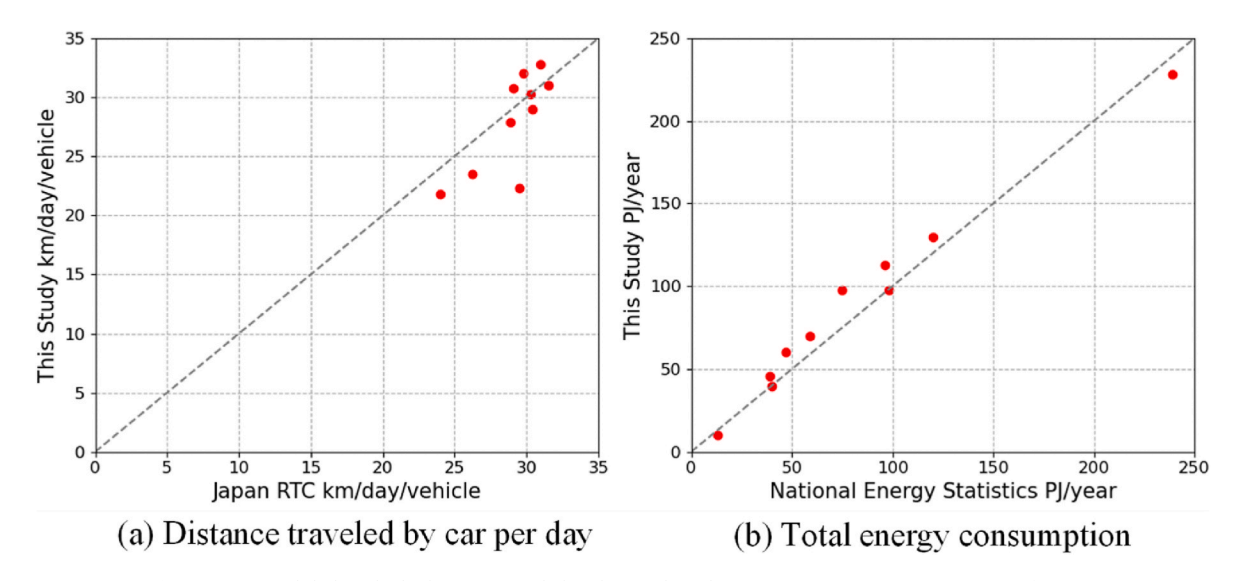


Fig. 6. Estimated daily vehicle distance traveled and annual total energy consumption in 10 regions of Japan.

generation and distribution networks. Figure B.1 shows the estimated EV charging demand overlaid on the actual electricity demand throughout Japan for the same period [43–52]. The total electricity demand would increase by an average of approximately 10 %, rising to approximately 30 % during peak times. The peak shape from the evening to the night would become sharper owing to the increase in EVs, and the peak time would be delayed by 1 h. These results indicate that EVs would have a significant impact on the total amount of electricity demand and its temporal characteristics.

3.4. Spatial variation in EV charging demand

To understand how the regional characteristics are reflected in the spatial distribution of charging demand, we analyzed the relationship with the accessibility to public transportation networks. In this study, we

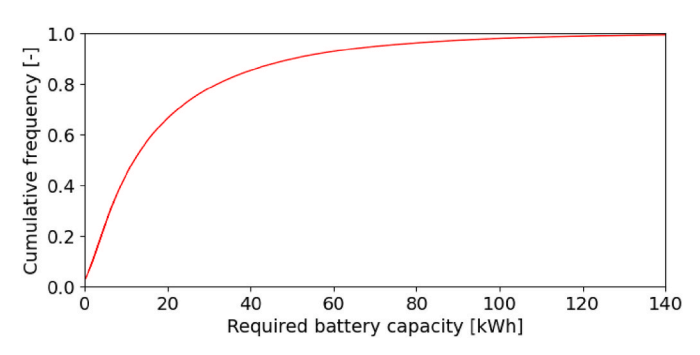


Fig. 7. Distribution of battery capacity required for uncontrolled charging.

used public transport accessibility level [53], PTAL, as an indicator of accessibility. Appendix C explains the method to quantify PTAL for each 1 km mesh from PTAL 1 to 6 (from the lowest to the highest accessibility) and mapped its spatial distribution.

Fig. 11 shows the estimated values of the charging demand per household in each PTAL. In PTALs 1, 2, and 3, the scale of charging demand was almost equal. However, the demand for charging decreased from PTAL 4. The peak demand for charging in PTAL 6 was

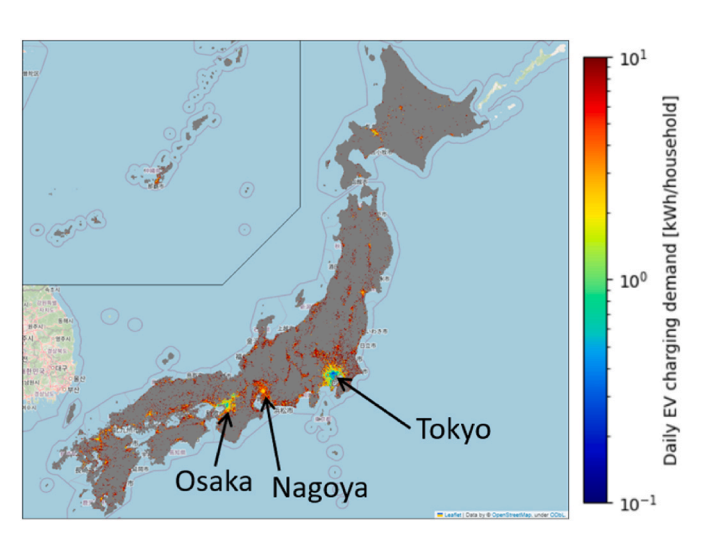


Fig. 8. Spatial distribution of daily charging demand.

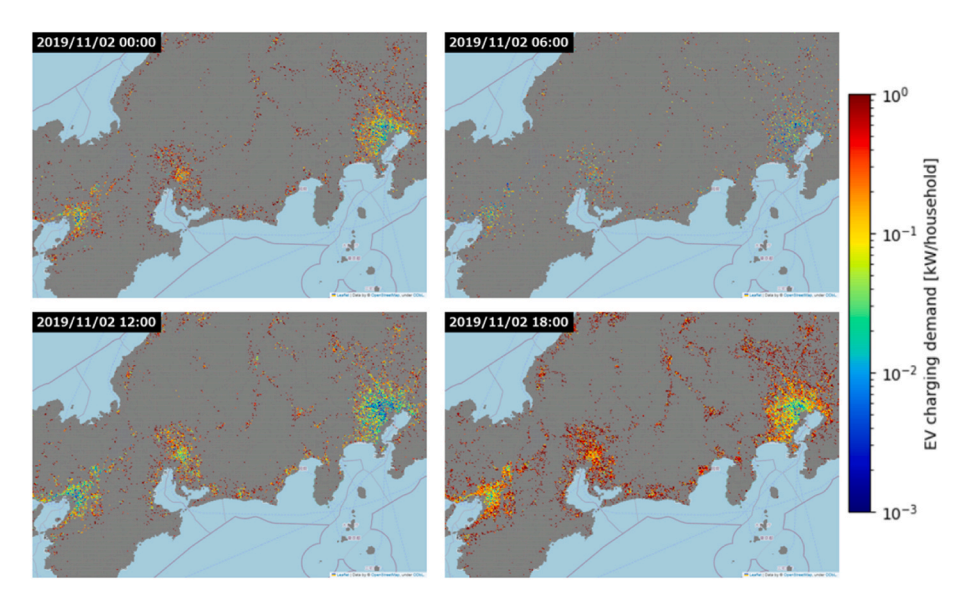


Fig. 9. Spatiotemporal distribution of charging demand on Saturday, November 2.

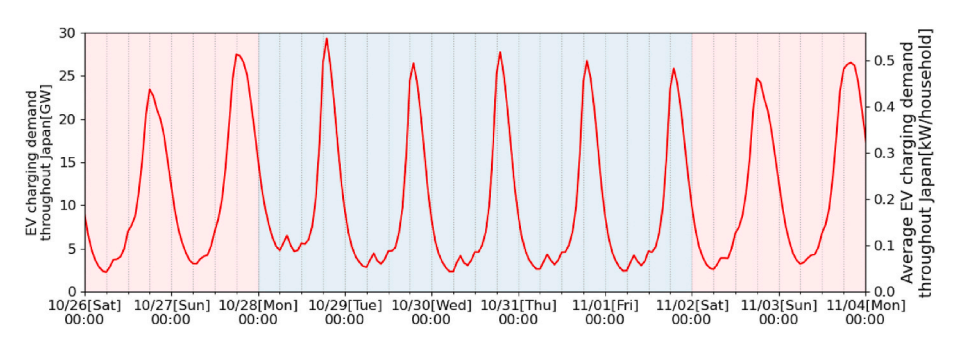


Fig. 10. Total charging demand from all EVs during uncontrolled charging periods. The background color indicates the distinction of weekdays (blue) or holidays (pink).

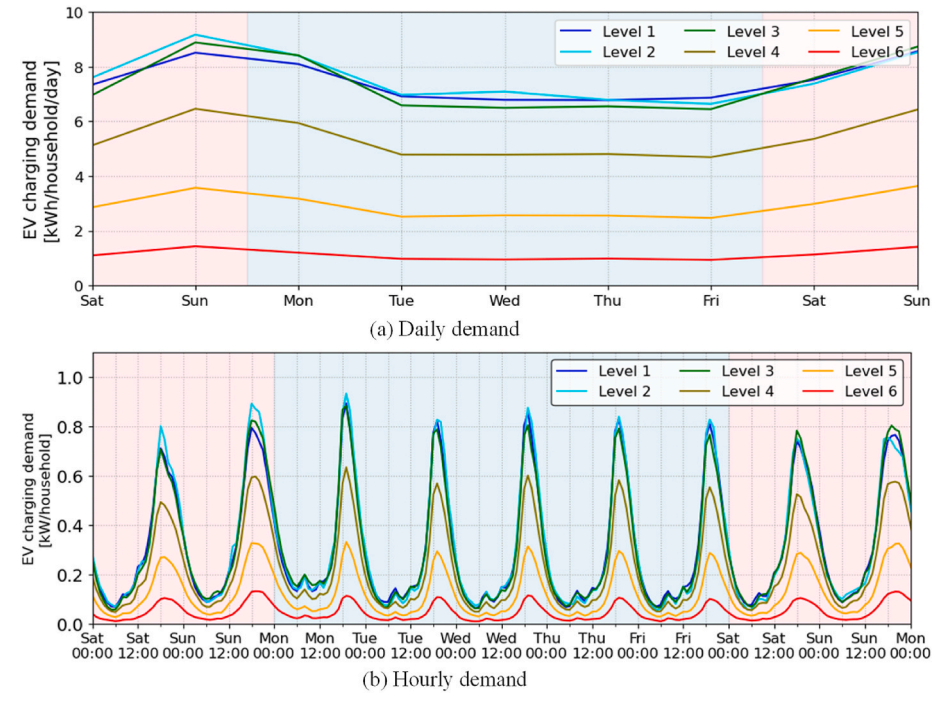


Fig. 11. Average EV charging demand per household in PTAL 1-PTAL 6: (a) daily and (b) hourly.

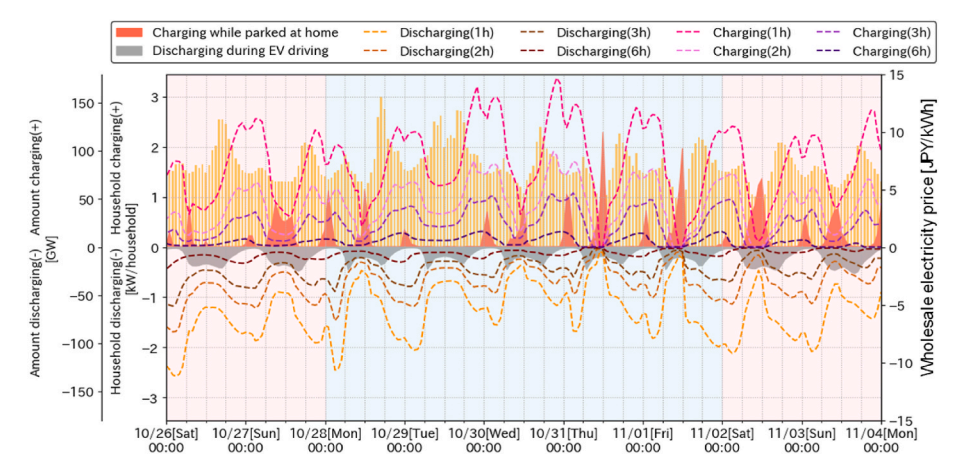


Fig. 12. Estimated total charging and discharging flexibility and per household. The gray area indicates the discharge by driving, whereas the red area indicates the charging demand with cost minimum charging (the electricity system price is shown by the orange bars). The charging and discharging flexibilities that can be provided by EV battery operation are shown by the lines for different charging/discharging durations.

approximately 10 % of the demand in PTAL 1. The daily demand on holidays, particularly on Sundays, was higher than that on weekdays. This trend was consistent across PTALs. The daily demand did not vary considerably from Tuesday to Friday. The temporal pattern shows no significant difference between PTALs, with the lowest demands at 4:00 and the highest demands at 19:00. The peak during the night is steeper on weekdays compared to weekends. This temporal pattern is obtained from the vehicle usage pattern shown in Figure C.2.

3.5. Estimation of flexibility

Fig. 12 shows the estimated charging and discharging flexibility of entire Japan. The flexibility was obtained based on the baseline condition (red area) that minimized operating costs. There were eight days when peak demand occurred around noon due to the impact of electricity prices. The flexibility indicated by the dotted lines decreases as the charging and discharging durations increase. In addition, when the electricity price is low, the potential for flexibility approaches zero because charging has been implemented in the baseline. Conversely, the potential for flexibility increases at night and early in the morning when the operating rate of EVs is low. In addition, the charging flexibility tends to attain its peak when EVs return to the living areas because the SOC is low. The discharging flexibility tends to attain its peak early in the morning, when the SOC is high before the EVs leave.

The charging flexibility for 6 h was estimated to be almost zero during the daytime when the output of solar photovoltaics becomes large because charging operations were assigned at the baseline, as mentioned above. The discharging flexibility for V2G during the evening peak between 17:00 and 19:00 was estimated to be 20 GW, 25 GW, and 50 GW for 3, 2, and 1 h on average. The discharging flexibility is larger

on weekdays than on holidays, and vice versa for the charging flexibility. Comparing peak values, charging flexibility on weekdays was 18 % higher than on holidays, while discharge flexibility on holidays was 16 % higher than on weekdays.

Fig. 13 shows the time-series variation in charging and discharging flexibility per household (assuming that the duration of charging and discharging is 1 h) by PTAL. In areas with PTAL 1 to PTAL 3, the charging and discharging flexibility barely differ. However, the peak value of charging and discharging flexibility decreases gradually from PTAL 4 to PTAL 6. Meanwhile, there is almost no variation in the time characteristics from PTAL 4 to PTAL 6. This is because as PTAL increases, the battery capacity allocated to EVs and the number of EVs that can be charged and discharged for flexibility decrease.

4. Discussion

4.1. Establishment of workflow

The workflow to extract vehicle usage from the low-quality location log data consists of classification tasks for stay-move state of logs, travel mode of trips, and location type of spots. Machine learning techniques were applied for these. The evaluation using annotated data described in Section 3.1 revealed that each task was performed with a high accuracy. The comparison in Section 3.2 reveals that the average travel distance per day and daily energy consumption of private vehicles agreed well with publicly available data. Although the spatial resolution was 10 Japanese regional divisions because of the data availability, it indicates that the developed model effectively represents the vehicle usage in Japan. Because of the method, large-scale data on vehicle usage were obtained from all over Japan at a high spatiotemporal resolution.

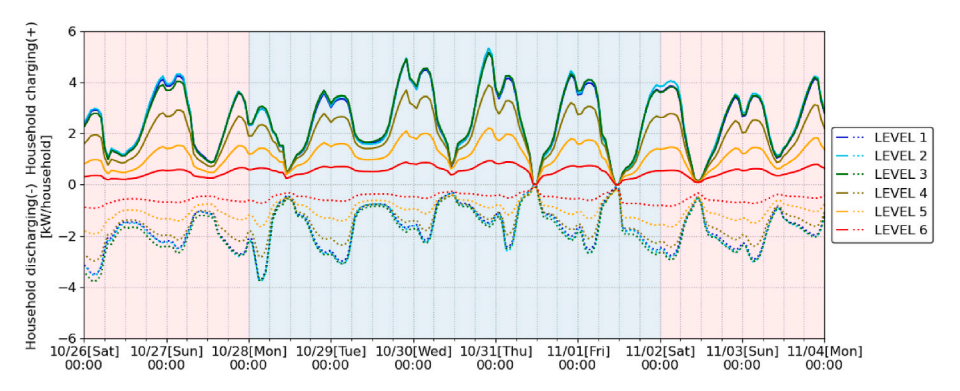


Fig. 13. Estimated total flexibility in PTAL 1-PTAL 6 with 1 h duration of charging and discharging.

However, a critical uncertainty remains on how well the location log data represents the vehicle usage of population. First, insufficient log samples were available in sparsely populated areas. Second, the location log data contains data that do not represent the user behavior appropriately as explained in Section 2.6. Therefore, only 20 % of users were sampled to obtain a good fit with the national survey data. Although the proportion of valid users is small, the thresholds selected in Table 2 are reasonable constraints to ensure data is removed that may not represent the actual behavior of users as shown in the distributions of the selected parameters in Supplementary Material D. We confirmed that the percentage of valid samples was 20.9 %, 21.7 %, 21.0 %, 17.9 %, 14.7 %, and 10.2 % for PTAL 1 (rural) to PTAL 6 (urban) areas, respectively. Appendix D compares the difference in charging demand by the sampling process and shows that omitting the sampling process significantly reduces total charging demand and peak charging demand. These results indicate that users with logs showing low frequency of movement outside the home mesh area were deleted more frequently, especially in urban areas. Although we used Bayesian optimization to determine the parameters to remove outlier users as in Table 2, a data-driven evaluation of valid users and days would be possible to increase the dataset used by machine learning methods trained with annotated data.

4.2. Data-driven spatiotemporal characterization of EV charging demand and flexibility

Despite location log data limitations, Sections 3.3–3.5. demonstrate the advantages of combining location log data with the DUOATS approach. It enables the quantification of the spatiotemporal characteristics of EV usage, charging demand, and flexibility at the national and local levels simultaneously. According to Section 3.3, the total charging demand reaches a maximum of 25 GW on both weekdays and holidays. The peak duration is longer during holidays than during weekdays. This indicates that the peak duration may be longer during summer and winter owing to the electricity demand for air-conditioning, because the observation in Shanghai revealed that the charging demand is two times higher than that in the other months [55]. Meanwhile, as shown in Section 3.5, EVs can provide significant charging flexibility for smart charging and discharging for V2G. Shifting evening charging demand to nighttime or daytime shown in the baseline operation in Fig. 12 helps alleviate evening peak loads. This also helps mitigate the impact of large-scale PV deployment during daytime. V2G operations can provide an additional 20 and 25 GW of discharge flexibility during evening peak hours for 3- and 2-h long discharge periods, respectively. On the other hand, additional daytime charging flexibility is limited when daytime charging is allocated in the baseline. We observed that the discharging flexibility is higher on weekdays than on holidays, and vice versa for the charging flexibility. Although we considered only private vehicles and home charging in this study, other places and company cars can be considered.

In Sections 3.4 and 3.5, the results reveal that the scale of charging demand and flexibility differs significantly among PTALs. However, their temporal patterns are similar. Although we used PTAL considering the accessibility to public transportation as the unit of analysis, it indicates that a detailed analysis can be performed at the local level to reflect the characteristics of EV usage and constraints for flexibility.

The proposed framework can generate the EV charging demand and flexibility across multiple spatial scales from a single vehicle at the household level to the city, prefectural, regional, and even national levels across the target area. These results reflect the regional characteristics and provide effective insights for power system planning at multiple scales.

4.3. Limitations and future works

Validation should be performed more comprehensively using available data sources. Furthermore, a more detailed analysis is required to

fully understand EV charging demand and flexibility. This is because the quantification process used several simplified assumptions regarding EV battery capacity (using maximum energy consumption during the period), charging behavior (assuming only uncontrolled charging), and flexibility participation scenarios (assuming that all vehicles are connected to the power grid while parked at home and always provide flexibility). These assumptions may have a significant impact on EV charging demand and flexibility. The presented workflow can be extended to analyze more realistic conditions and diverse charging and flexibility scenarios (e.g., charging/discharging at workplaces and other locations, commercial vehicle cases, etc.).

As explained in Section 4.1, the impact of user sampling on estimation results should be better understood. This is particularly important for the accurate representation of sparsely populated areas where the availability of original data is generally low. In this paper, we merged such areas with neighboring areas. Furthermore, methods should be established to fully use available location logs. A potential method is to develop an ABM based on developed activity data combined with other data sources. Owing to the unavailability of demographic information in the location log, the integrated use with travel survey data would be advantageous [20]. Location log data would contribute to better characterizing the spatiotemporal features of user behavior in ABMs. The development of an ABM considering a synthetic population provides flexible applications to take into account different periods and future situations. This, in turn, would enable a more integrated analysis with the energy demands of building sectors [30] and power systems [5]. In addition, this study relied on mobility trajectories observed under existing conditions. It did not incorporate the potential variations in vehicle usage and ownership because of vehicle electrification and automation or variations in the availability and accessibility of charging infrastructure. Future research should address these behavioral responses.

5. Conclusion

Location log big data collected from mobile devices has a significant potential to enhance the spatiotemporal resolution in modeling EV usage, battery charging demand, and flexibility. Notwithstanding its potential, no research has been conducted on using location log big data to model these elements on a large scale at a high spatiotemporal resolution. This study established a data-driven workflow to extract vehicle activity schedules from location log data and directly used the extracted activity schedules to quantify the vehicle usage, EV charging demand, and flexibility at the national and local levels while considering the local activity characteristics and constraints. The workflow was validated at the log and individual levels with annotated data and at the aggregated level with average distance traveled per day and annual energy consumption from subnational-level statistics. The result showed that the EV charging demand in Japan would reach a maximum of 25 GW in mid seasons with uncontrolled charging on both weekdays and holidays. The peak durations are longer on holidays than on weekdays, and an increase in energy consumption causes an increase in peak durations. The activity patterns, demand, and flexibility significantly vary with the accessibility to public transportation. The results demonstrate that the established method can provide high spatiotemporal resolution EV data for various power system analyses while considering common scenarios in terms of EV deployment, charging schedule, and flexibility operation. Additionally, it allows for iterative studies that integrate local and macro-level power systems. Further research is required to integrate spatiotemporal characteristics obtained from location log data with activity-based vehicle usage models to fully utilize the potential of location log data.

CRediT authorship contribution statement

Yohei Yamaguchi: Writing - review & editing, Writing - original

draft, Methodology, Funding acquisition, Formal analysis, Conceptualization. Yudai Ochi: Writing – original draft, Validation, Methodology, Investigation, Formal analysis. Ryotaro Ohara: Writing – original draft, Validation, Methodology, Investigation, Formal analysis. Hideaki Uchida: Writing – review & editing, Methodology, Conceptualization. Shinya Yoshizawa: Writing – review & editing, Methodology, Conceptualization. Katsuya Sakai: Writing – review & editing, Methodology, Conceptualization. Yutaka Ota: Writing – review & editing, Resources, Project administration, Methodology, Funding acquisition, Conceptualization. Yoshiyuki Shimoda: Writing – review & editing, Supervision, Resources, Project administration, Funding acquisition, Conceptualization.

Funding

This work was supported by JSPS KAKENHI Grant Numbers 23K26260 and 23K13311.

Declaration of competing interest

The authors declare that they have no known competing financial interests or personal relationships that could have appeared to influence the work reported in this paper.

Appendices.

Appendix A. Machine learning models used for classification processes

A.1. Machine learning model for travel mode classification

The features listed in Table A.1 were considered in the model development. Supplementary Material B.1 provides details of the features.

Table A.1Features used for classifying travel mode

Feature	Low-quality trips	High-quality trips
Average speed	√	√
Variance of speed		✓
85th percentile of speed	✓	✓
Average acceleration		✓
Variance of acceleration		✓
85th percentile of acceleration		✓
Average turning angular velocity		✓
Variance of turning angular velocity		✓
85th percentile of turning angular velocity		✓
Percentage of logs with low speed	✓	✓
Number of logs	✓	✓
Route length	✓	✓
Linear distance	✓	✓
Ratio of linear distance to route length	✓	✓
Concordance rate with train mesh	✓	✓
Number of airports passed through	✓	✓
Concordance rate with sea mesh	✓	✓
Transportation for previous high-quality trip	✓	
Transportation for next high-quality trip	✓	

A.2. Machine learning model for spot classification

The XGBoost model calculated the probability that the spot was the user's living area or working area. One kilometer mesh of the spot with the highest probability of being the user's living area was considered as their living area. Then, among the spots other than the living area, 1 km mesh of the spot with the highest probability of being the working area was considered to be the working area (among the spots with a workplace probability of at least 0.5). Users who did not have a workplace probability of at least 0.5 at any of the spots other than their living area were considered to be non-commuters. Table A.2 lists the features considered in the XGBoost model. Supplementary Material B.1 provides details of the features. Spots that users have visited only one time cannot be classified because the variance of arrival and departure times cannot be calculated. Moreover, it was assumed that most individuals stayed in living or working areas at least two times within 12 days.

Table A.2 Feature values for classifying stay points

Feature value	Living area	Working area	
Number of days visited	✓	✓	
Total time spent	✓	✓	
Average arrival time	✓	✓	
Variance of arrival time	✓	✓	
Average departure time	✓	✓	
Variance of departure time	✓	✓	
Population of 1 km mesh	✓		
Distance from living area		✓	

Appendix B. EV charging demand

Figure B.1 shows the estimated EV charging demand with the uncontrolled charging overlaid on the actual electricity demand throughout Japan for the same period [43–52].

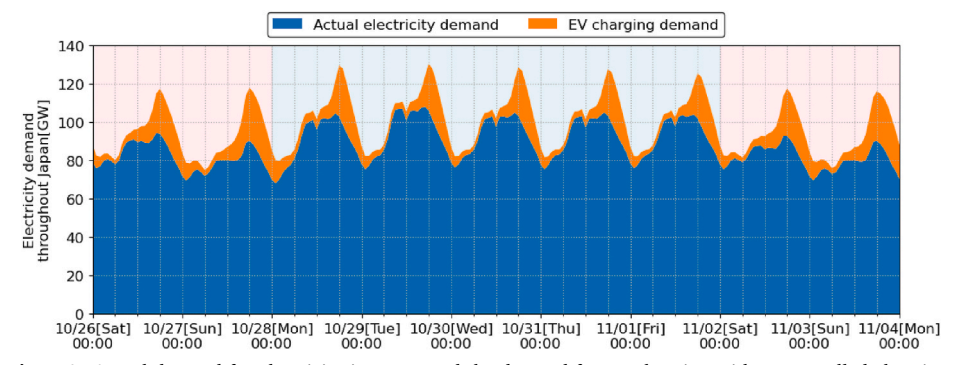


Fig. B.1. Actual demand for electricity in Japan and the demand for EV charging with uncontrolled charging.

Appendix C. PTAL

The accessibility index AI for each mesh was calculated as in Eq. (C.1) based on two factors¹: the walk time WT from each mesh to the nearby train station or bus stop, and the average waiting time at the stations SWT.

$$AI_{mesh} = \sum_{Station} \frac{1}{WT + SWT}$$
 (C.1)

WT was calculated by increasing the straight-line distance from the center point of the mesh to the station by 30 % to account for the differences from the actual route, and then dividing by the assumed walking speed of 5 km/h. *SWT* was expressed as the average time interval between trains and buses departing from each station. ² *Stations* are those within a 3 km radius from the center point of the target mesh.

The distribution of AI_{mesh} is shown in Figure C.1(a). As illustrated in Figure C.1(b), the distribution fits the lognormal distribution well. Thus, the meshes were classified into six PTALs using the mean μ and standard deviation σ of the lognormal distribution fitted by the maximum likelihood estimation method excluding those where AI_{mesh} was 0 as PTAL = 1 where $AI_{mesh} < \mu - 2\sigma$, the least accessible areas, to PTAL = 6 where $AI_{mesh} > \mu + 2\sigma$, the most convenient meshes as Level 6.

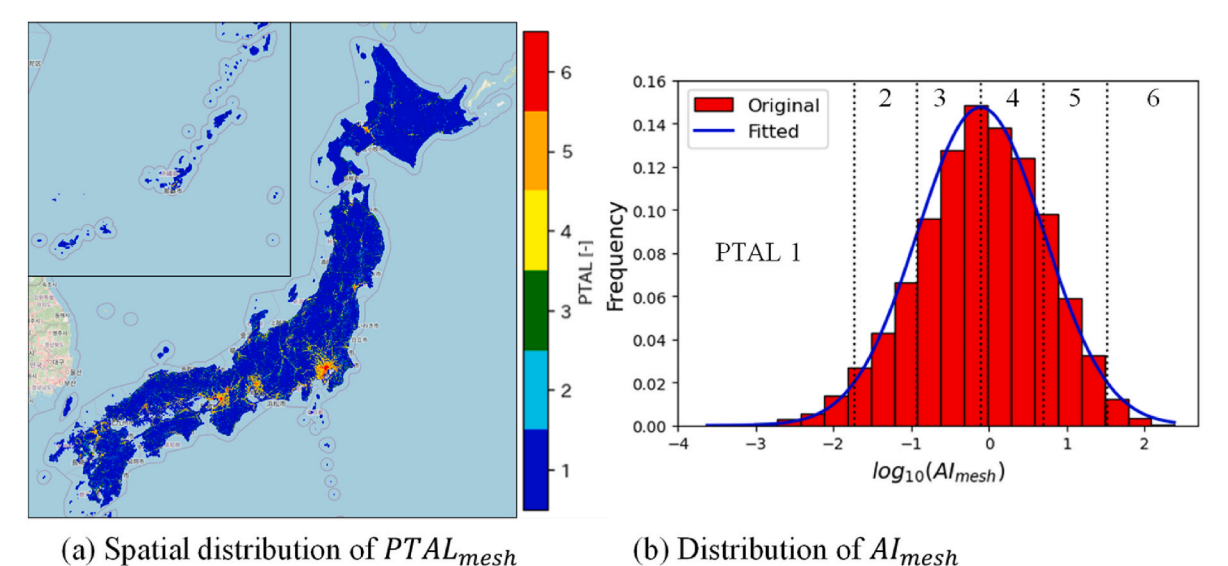


Fig. C.1. Distribution of PTAL_{mesh} and AI_{mesh}

Figure C.2 presents the percentage of vehicles in motion, charging, or parked in living areas in PTALs 1 and 6. Vehicles are parked in living areas for longer periods in PTAL 6 than in PTAL 1, wherein vehicles are parked longer in working area or other spots.

¹ Unlike the original concept underlying the AI calculation formula, the reliability coefficient was not considered because of the high reliability of Japan's public transportation system.

² The daytime service frequency data of train stations is a dataset [54]. The data source is the 2019 timetable. The data include the number of passenger trains arriving and leaving stations between 10:00 and 17:00 on weekdays.

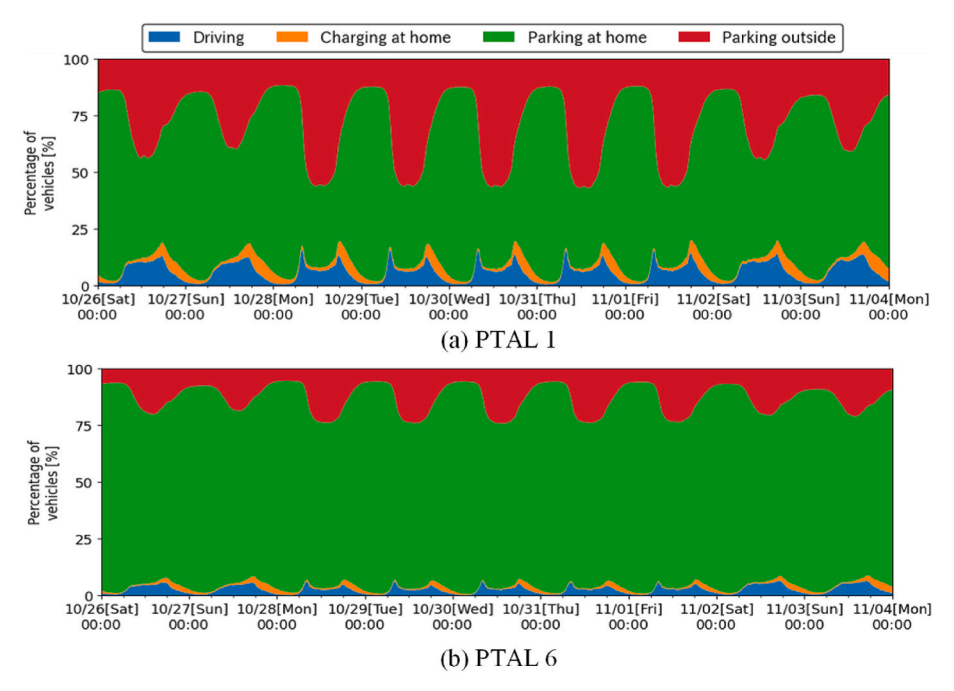


Fig. C.2. Composition of the state of vehicle under uncontrolled charging in (a) PTAL 1 and (b) PTAL 6.

Appendix D. Charging demand estimated with all location log

Figure D.1 shows the difference in charging demand under the uncontrolled charging with/without the sampling process. The peak became half, and the total charging demand decreased by 46 % compared with the case with sampling.

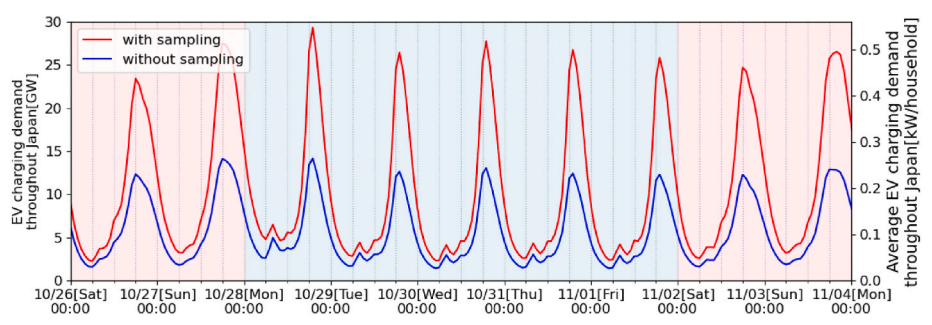


Fig. D.1. Comparison of charging demand with/without the sampling process.

Appendix A. Supplementary data

Supplementary data to this article can be found online at https://doi.org/10.1016/j.energy.2025.137804.

Data availability

The authors do not have permission to share data.

References

- [1] Salah F, Ilg JP, Flath CM, Basse H, Dinther C van. Impact of electric vehicles on distribution substations: a Swiss case study. Appl Energy 2015;137:88–96. https://doi.org/10.1016/j.apenergy.2014.09.091.
- [2] Gupta R, Pena-Bello A, Streicher KN, Roduner C, Thöni D, Patel MK, et al. Spatial analysis of distribution grid capacity and costs to enable massive deployment of PV, electric mobility and electric heating. Appl Energy 2021;287:116504. https:// doi.org/10.1016/J.APENERGY.2021.116504.
- [3] Boßmann T, Staffell I. The shape of future electricity demand: exploring load curves in 2050s Germany and Britain. Energy 2015;90:1317–33. https://doi.org/ 10.1016/j.energy.2015.06.082.

- [4] Richardson DB. Electric vehicles and the electric grid: a review of modeling approaches, Impacts, and renewable energy integration. Renew Sustain Energy Rev 2013;19:247–54. https://doi.org/10.1016/j.rser.2012.11.042.
- [5] Vollmuth P, Wohlschlager D, Wasmeier L, Kern T. Prospects of electric vehicle V2G multi-use: profitability and GHG emissions for use case combinations of smart and bidirectional charging today and 2030. Appl Energy 2024;371:123679. https://doi.org/10.1016/j.apenergy.2024.123679.
- [6] Kataoka R, Ogimoto K, Iwafune Y, Nishi T. Changing role of battery electric vehicle charging strategies in decarbonizing Japanese power systems. Energy 2025;327: 136413. https://doi.org/10.1016/J.ENERGY.2025.136413.
- [7] Daina N, Sivakumar A, Polak JW. Modelling electric vehicles use: a survey on the methods. Renew Sustain Energy Rev 2017;68:447–60. https://doi.org/10.1016/j. rser.2016.10.005.
- [8] Li X, Wang Z, Zhang L, Sun F, Cui D, Hecht C, Figgener J, Sauer DU. Electric vehicle behavior modeling and applications in vehicle-grid integration: an overview. Energy 2023;268. https://doi.org/10.1016/j.energy.2023.126647.
- [9] Patil P, Kazemzadeh K, Bansal P. Integration of charging behavior into infrastructure planning and management of electric vehicles: a systematic review

- and framework. Sustain Cities Soc 2023;88:104265. https://doi.org/10.1016/J.
- [10] Mu Y, Wu J, Jenkins N, Jia H, Wang C. A Spatial-Temporal model for grid impact analysis of plug-in electric vehicles. Appl Energy 2014;114:456–65. https://doi. org/10.1016/j.apenergy.2013.10.006.
- [11] Mangipinto A, Lombardi F, Sanvito FD, Pavičević M, Quoilin S, Colombo E. Impact of mass-scale deployment of electric vehicles and benefits of smart charging across all European countries. Appl Energy 2022;312. https://doi.org/10.1016/j. apenergy.2022.118676.
- [12] Lin H, Fu K, Wang Y, Sun Q, Li H, Hu Y, Sun B, Wennersten R. Characteristics of electric vehicle charging demand at multiple types of location - application of an agent-based trip chain model. Energy 2019;188. https://doi.org/10.1016/j. energy 2019 116122
- [13] Jahangir H, Tayarani H, Ahmadian A, Golkar MA, Miret J, Tayarani M, Gao HO. Charging demand of plug-in electric vehicles: forecasting travel behavior based on a novel rough artificial neural network approach. J Clean Prod 2019;229:1029–44. https://doi.org/10.1016/j.jclepro.2019.04.345.
- [14] Zhang J, Yan J, Liu Y, Zhang H, Lv G. Daily electric vehicle charging load profiles considering demographics of vehicle users. Appl Energy 2020;274. https://doi. org/10.1016/j.apenergy.2020.115063.
- [15] Pareschi G, Küng L, Georges G, Boulouchos K. Are travel surveys a good basis for EV models? Validation of simulated charging profiles against empirical data. Appl Energy 2020;275. https://doi.org/10.1016/j.apenergy.2020.115318.
- [16] Liu YS, Tayarani M, Gao HO. An activity-based travel and charging behavior model for simulating battery electric vehicle charging demand. Energy 2022;258. https:// doi.org/10.1016/j.energy.2022.124938.
- [17] Gschwendtner C, Knoeri C, Stephan A. The impact of plug-in behavior on the spatial-temporal flexibility of electric vehicle charging load. Sustain Cities Soc 2023;88. https://doi.org/10.1016/j.scs.2022.104263.
- [18] Szinai JK, Sheppard CJR, Abhyankar N, Gopal AR. Reduced grid operating costs and renewable energy curtailment with electric vehicle charge management. Energy Policy 2020;136:111051. https://doi.org/10.1016/J.ENPOL.2019.111051.
- [19] Wu J, Powell S, Xu Y, Rajagopal R, Gonzalez MC. Planning charging stations for 2050 to support flexible electric vehicle demand considering individual mobility patterns. Cell Reports Sustainability 2024;1(1):100006. https://doi.org/10.1016/ J.CRSUS.2023.100006.
- [20] Fischer D, Harbrecht A, Surmann A, McKenna R. Electric vehicles' impacts on residential electric local profiles – a stochastic modelling approach considering socio-economic, behavioural and spatial factors. Appl Energy 2019;233–234: 644–58. https://doi.org/10.1016/j.apenergy.2018.10.010.
- [21] Muratori M. Impact of uncoordinated plug-in electric vehicle charging on residential power demand. Nat Energy 2018;3(3):193–201. https://doi.org/ 10.1038/s41560-017-0074-z.
- [22] Müller M, Biedenbach F, Reinhard J. Development of an integrated simulation model for load and mobility profiles of private households. Energies 2020;13(15): 3843. https://doi.org/10.3390/EN13153843, 2020, Vol. 13, Page 3843.
- [23] Auld J, Cook J, Gurumurthy KM, Khan N, Mansour C, Rousseau A, Sahin O, de Souza F, Verbas O, Zuniga-Garcia N. Large-scale evaluation of mobility, technology and demand scenarios in the Chicago region using POLARIS. https://arxiv.org/abs /2403.1466991. 2024
- [24] Rostami A, Verbas O, Ghafarnezhad B, Soltanpour A, Ghamami M, Zockaie A. Exploring impacts of electricity tariff on charging infrastructure planning: an activity-based approach. Transport Res Transport Environ 2024;136:104451. https://doi.org/10.1016/J.TRD.2024.104451.
- [25] Huang L, Xia F, Chen H, Hu B, Zhou X, Li C, Jin Y, Xu Y. Reconstructing human activities via coupling mobile phone data with location-based social networks. Travel Behaviour and Society 2023;33:100606. https://doi.org/10.1016/J. TBS.2023.100606.
- [26] Liu Y, Dong B. Modeling urban scale human mobility through big data analysis and machine learning. Build Simul 2024;17:3–21. https://doi.org/10.1007/S12273-023-1043-Z/METRICS
- [27] Martin H, Hong Y, Wiedemann N, Bucher D, Raubal M. Trackintel: an open-source Python library for human mobility analysis. Comput Environ Urban Syst 2023;101: 101938. https://doi.org/10.1016/J.COMPENVURBSYS.2023.101938.
- [28] Xu Y, Çolak S, Kara EC, Moura SJ, González MC. Planning for electric vehicle needs by coupling charging profiles with urban mobility. Nat Energy 2018;3(6):484–93. https://doi.org/10.1038/s41560-018-0136-x. 2018 3:6.
- [29] Zhang H, Song X, Xia T, Yuan M, Fan Z, Shibasaki R, et al. Battery electric vehicles in Japan: human mobile behavior based adoption potential analysis and policy target response. Appl Energy 2018;220:527–35. https://doi.org/10.1016/j. apenergy.2018.03.105.
- [30] Zhang H, Chen J, Yan J, Song X, Shibasaki R, Yan J. Urban power load profiles under ageing transition integrated with future EVs charging. Adv Appl Energy 2021;1:100007. https://doi.org/10.1016/J.ADAPEN.2020.100007.
- [31] Agoop. Agoop location log data. https://agoop.co.jp/service/dynamic-populat ion-data/. [Accessed 15 April 2025].
- [32] Zheng Y. Trajectory data mining. ACM Transactions on Intelligent Systems and Technology (TIST) 2015;6(3). https://doi.org/10.1145/2743025.

- [33] Gong L, Yamamoto T, Morikawa T. Identification of activity stop locations in GPS trajectories by DBSCAN-TE method combined with support vector machines. Transp Res Procedia 2018;32:146–54. https://doi.org/10.1016/J. TRPRO 2018 10 028
- [34] Ministry of Land, Infrastructure, and Transport Road Bureau. National road and Street traffic conditions survey in 2015. https://www.e-stat.go.jp/stat-search/files?page=1&layout=datalist&toukei=00600580&tstat=000001116435&cycle=8&tclass1=000001138689&tclass2=000001138690&tclass3val=0;2021. [Accessed 15 April 2025].
- [35] Japan Vehicle Inspection and Registration Information Association. Statistics on the number of vehicles owned 2020. https://www.airia.or.jp/publish/book/edata. html. 15 Apr 2025.
- [36] Japan Mini Vehicles Association. Number of light vehicles by municipality. As of March 31, 2023, No.45, https://www.zenkeijikyo.or.jp/statistics/book. [Accessed 15 April 2025].
- [37] Yamaguchi Y, Miyahara K, Ochi Y, Ohara R, Ota Y, Uchida H, Shimoda Y. Activity-based synthetic framework for modelling energy demand of residential building stock. In: Proceedings BS2023; 2023. p. 2744–51. https://doi.org/10.26868/25222708.2023.1542.
- [38] Iwafune Y., Ogimoto K., Kobayashi Y., Murai K. Driving Simulator for Electric Vehicles Using the Markov Chain Monte Carlo Method and Evaluation of the Demand Response Effect in Residential Houses. IEEE Access 8, 47654–47663. https://doi.org/10.1109/ACCESS.2020.2978867.
- [39] Japan Electric Power Exchange. Database of wholesale electricity price. htt ps://www.jepx.jp/electricpower/market-data/spot/. [Accessed 15 April 2025]
- [40] Yang X, Stewart K, Tang L, Xie Z, Li Q. A review of GPS trajectories classification based on transportation mode. Sensors 2018;18(11):3741. https://doi.org/ 10.3390/S18113741. 2018, Vol. 18, Page 3741.
- [41] Agency for Natural Resources and Energy [Internet]. Tokyo: Ministry of Economy. Trade and industry. General Energy Statistics 2023. https://www.enecho.meti.go. jp/statistics/total_energy/results.html#headline7. [Accessed 15 April 2025]. Japanese.
- [42] Ministry of Land, Infrastructure, and Transport. Trends in average JC08 mode fuel efficiency for gasoline-powered passenger cars. https://www.mlit.go.jp/jidosha/content/3.2.R3_LDFE_JC08.pdf. [Accessed 15 April 2025]. Japanese.
- [43] Hokuden Network. Downloading past electricity usage data Hokuden Network. https://denkiyoho.hepco.co.jp/area download.html. 2024/01/21.
- [44] Tohoku Electric Power Network. Downloading historical data | Tohoku electric power network. https://setsuden.nw.tohoku-epco.co.jp/download.html. [Accessed 15 April 2025].
- [45] Tokyo Electric Power Grid; Historical electricity usage data Explanation of electricity forecasts Tokyo Electric Power Holdings, Inc., https://www.tepco.co.jp/ forecast/html/download-j.html, [accessed 15 April 2025].
- [46] Chubu Electric Power Grid; Electricity Forecast Chubu Electric Power Grid, htt ps://powergrid.chuden.co.jp/denkiyoho/, [accessed 15 April 2025].
 [47] Hokuriku Electric Power Transmission and Distribution; Area Supply and Demand
- [47] Hokuriku Electric Power Transmission and Distribution; Area Supply and Demand Results, Hokuriku Electric Power Transmission and Distribution, https://www. rikuden.co.jp/nw_jyukyudata/area_jisseki.html, [accessed 15 April 2025].
- [48] Kansai Electric Power Transmission and Distribution; Downloading historical electricity usage data | Electricity Forecasting | Kansai Electric Power Transmission and Distribution Co., https://www.kansai-td.co.jp/denkiyoho/download/index. html, [accessed 15 April 2025].
- [49] Chugoku Electric Power Network; Electricity Forecast Chugoku Electric Power Network, https://www.energia.co.jp/nw/jukyuu/, [accessed 15 April 2025].
- [50] Shikoku Electric Power Transmission and Distribution; Downloading past usage data|Shikoku Electric Power Transmission and Distribution, https://www.yonden. co.jp/nw/denkiyoho/download.html, [accessed 15 April 2025].
- [51] Kyushu Electric Power Transmission and Distribution; Kyushu Electric Power Transmission and Distribution Electricity Forecast (Electricity Usage Status), http s://www.kyuden.co.jp/td_power_usages/pc.html, [accessed 15 April 2025].
- [52] Okinawa Electric Power Company. Past electricity usage Results Electricity Forecast Okinawa electric power company. https://www.okiden.co.jp/denki2/dl/. [Accessed 15 April 2025].
- [53] Transport for London's. Assessing transport connectivity in London. https://data. london.gov.uk/dataset/public-transport-accessibility-levels. [Accessed 15 April 2025].
- [54] Nishizawa A. Data on the number of trains in operation during the daytime. http s://gtfs-gis.jp/station/. [Accessed 15 April 2025].
- [55] Qin Y, Dai Y, Huang J, Xu H, Lu L, Han X, Du J, Ouyang M. Charging patterns analysis and multiscale infrastructure deployment: based on the real trajectories and battery data of the plug-in electric vehicles in Shanghai. J Clean Prod 2023; 425:138847. https://doi.org/10.1016/J.JCLEPRO.2023.138847.
- [57] Yaghoubi E, Yaghoubi E, Khamees A, Razmi D, Lu T. A systematic review and metaanalysis of machine learning, deep learning, and ensemble learning approaches in predicting EV charging behavior. Eng Appl Artif Intell 2024;135:108789. https:// doi.org/10.1016/J.ENGAPPAI.2024.108789.